Proc. NIPR Symp. Upper Atmos. Phys., 1, 153–167, 1988

OCCURRENCE MAP OF BROAD-BAND AURORAL VLF HISS OBSERVED BY ISIS SATELLITES

Tadanori ONDOH

Radio Research Laboratory, 2–1, Nukui-Kitamachi 4-chome, Koganei-shi, Tokyo 184

Abstract: A polar map of occurrence rate of broad-band auroral VLF hiss is drawn by using narrow-band VLF intensity data of 6 frequencies which were processed from ISIS electric field (50 Hz–30 kHz) tapes of 347 passes received at Syowa Station, Antarctica from June 1976 to January 1983.

The high-latitude contour of occurrence rate of 0.3 lies at invariant latitude of about 82° for all local times. The low-latitude contour of 0.3 lies at 74° around 10 h geomagnetic local time (MLT) and it extends down to 67° around 22 h MLT, showing a symmetricity with respect to the 10–22 h MLT meridian. Two regions of high occurrence rate above 0.5 lie between 76° and 78° in the afternoon sector and also between 78° and 81° in the late night-morning sector. The result is not consistent with the occurrence map of auroral hiss at 9.6 kHz with a pronounced dawn-dusk asymmetry obtained from Ariel magnetic field data by HUGHES *et al.* (Space Research XI, ed. by K. Ya. KONDRATYEV *et al.* Berlin, Akademie, 1323–1330, 1971). This discrepancy between the ISIS and Ariel results is discussed from view points of auroral particle precipitation and difference in VLF data used.

1. Introduction

Ground-based observations of VLF radio noises at high latitudes show that intense bursts of broad-band VLF radio noises occur often in association with auroral disturbances (ELLIS, 1957; DUNCAN and ELLIS, 1959; MARTIN *et al.*, 1960; JØRGENSEN and UNGSTRUP, 1962; ONDOH, 1963; MOROZUMI, 1963; HARANG and LARSEN, 1965). These VLF emissions were classified as auroral hiss by HELLIWELL (1965). GURNETT (1966) first reported satellite observations of auroral hiss associated with precipitating electrons of energies below 10 keV. Correlative analyses of satellite data (GURNETT and FRANK, 1972; HOFFMAN and LAASPERE, 1972) have firmly established that auroral hiss is generated by intense fluxes of precipitating auroral electrons with energies from a few hundred eV to several keV.

HUGHES *et al.* (1971) reported the spatial distribution of occurrence frequency of auroral hiss with magnetic field intensity above 10^{-12} gamma^2 Hz^{-1} at 9.6 kHz over the polar region using the Ariel VLF magnetic field data. In this distribution, the maximum occurrence of auroral hiss closely follows the auroral oval, varying from about 80° invariant latitude on the dayside of the earth to about 72° invariant latitude on the nightside of the earth, and a pronounced dawn-dusk asymmetry is clearly evident, with a distinct minimum in the auroral hiss occurrence in the local morning from about 2 to 8 h geomagnetic local time. The morning minimum in the auroral hiss occurrence seems to be unreal since the auroral hiss is actually often observed by

ISIS satellites in the dawn to morning sector of the auroral oval. So, in this paper, we examine statistically the polar distribution of occurrence frequency of the broad-band auroral hiss using VLF electric field data (50 Hz–30 kHz) of ISIS-1 and ISIS-2 received at Syowa Station (geomag. lat. 69.7°S, long. 77.7°E), Antarctica.

2. Broad-band Auroral Hiss Observed in the Local Morning of Polar Region

We analyze narrow-band VLF data of ISIS satellites received at Syowa Station, Antarctica as shown in Figs. 1a–1c in order to examine the district minimum in the auroral hiss occurrence in the local morning of polar region. The maximum range in intensity variation of narrow-band VLF data is about 30 dB in arbitrary scale, while the range of light and shade of our $f-t$ spectrum films is, at most, about 10 dB. So, we can detect more auroral hisses in the narrow-band VLF data than the VLF $f-t$ spectrum films. The narrow-band VLF data of ISIS satellites compiled in the Radio and Space Data Nos. 9, 13 and 15 are processed from DR outputs of ISIS-VLF electric field (50 Hz–30 kHz) tapes by narrow-band DC amplifiers with a minimum reading circuit similar to a typical VLF hiss receiver used at ground stations in the auroral zone. Charging and discharging time constants of the minimum reading circuits are 10 s and 10 ms respectively. VLF output signals from the minimum reading circuit are compressed by a logarithmic DC amplifier for chart-recording. Figures 1a–1c show time or spatial variations of ISIS-VLF electric fields at 6 fixed frequencies of 300 Hz, 1.5, 5, 8, 16 and 20 kHz received at Syowa Station on October 31, 1978 ($Kp=2+$), February 5, 1977 ($Kp=4-$) and February 11, 1977 ($Kp=8+$), respectively.

Broad-band auroral hisses appearing at 5, 8, 16 and 20 kHz channels are seen respectively from 04 to 07 h in geomagnetic local time (MLT) on October 31, 1978 ($Kp=2+$) between invariant latitudes of 73° and 75° (Fig. 1a), from 05 to 09 h MLT on February 5, 1977 ($Kp=4-$) between 73° and 75° (Fig. 1b) and from 05 to 08 h MLT on February 11, 1977 ($Kp=8+$) between 72° and 75° (Fig. 1c). Thus, intense broad-band auroral hisses were clearly observed by ISIS satellites in the local morning in the polar region for various geomagnetic activities. This result is not consistent with the distinct minimum in the auroral hiss occurrence in the local morning found by HUGHES *et al.* (1971). The occurrence map of auroral hiss at 9.6 kHz obtained by HUGHES *et al.* (1971) shows actually no occurrence of auroral hiss between 05 and 06 h MLT in high latitudes.

In the next section, we examine statistically the spatial and time distribution of the occurrence rate of broad-band auroral hiss in high latitudes using ISIS-VLF data with a wide latitudinal extent received at Syowa Station, Antarctica.

3. Polar Map of Occurrence Rate of Broad-band Auroral Hiss Obtained from ISIS-VLF Data

The Syowa Station, Antarctica is suitable for collecting VLF data of polar orbiting ISIS satellites to make a polar occurrence map of the auroral hiss, since the latitudinal extent of telemetry coverage for ISIS satellites by Syowa Station is more

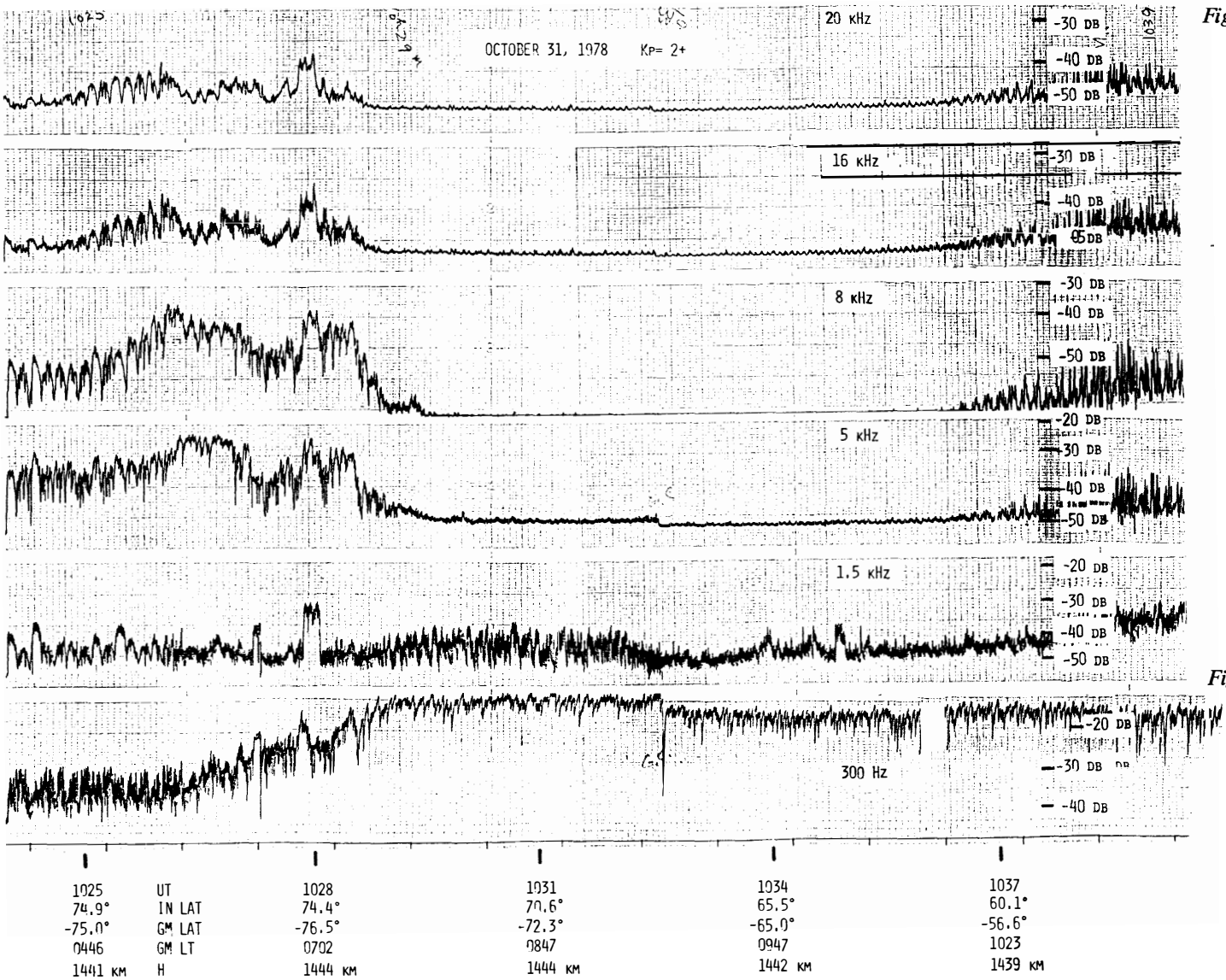

Fig. 1a.

Figs. 1a– 1c. Examples of broad-band auroral hisses (intensity increases at 5, 8, 16 and 20 kHz bands observed in the local morning at high latitudes on October 31, 1978, Kp=2+ (1a), February 5, 1977, Kp= 4− (1b) and February 11, 1977, Kp=8+ (1c) by the ISIS-2.

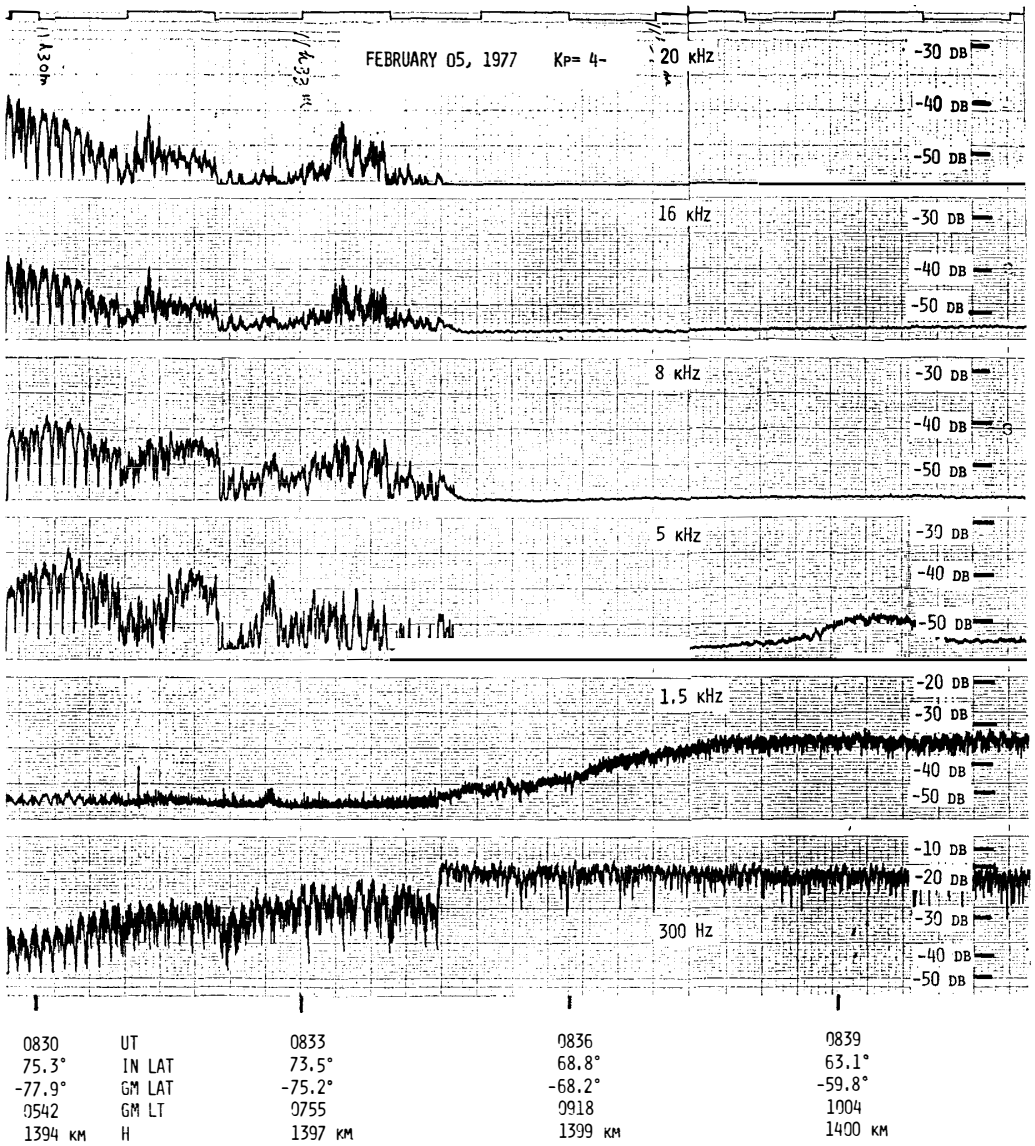
FEBRUARY 05, 1977 Kp= 4-
20 kHz
-30 DB
-40 DB
-50 DB
16 kHz
-30 DB
-40 DB
-50 DB
8 kHz
-30 DB
-40 DB
-50 DB
5 kHz
-30 DB
-40 DB
-50 DB
1.5 kHz
-20 DB
-30 DB
-40 DB
-50 DB
300 Hz
-10 DB
-20 DB
-30 DB
-40 DB
-50 DB
0830 UT 0833 0836 0839
75.3° IN LAT 73.5° 68.8° 63.1°
-77.9° GM LAT -75.2° -68.2° -59.8°
0542 GM LT 0755 0918 1004
1394 KM H 1397 KM 1399 KM 1400 KM

Fig. 1b.

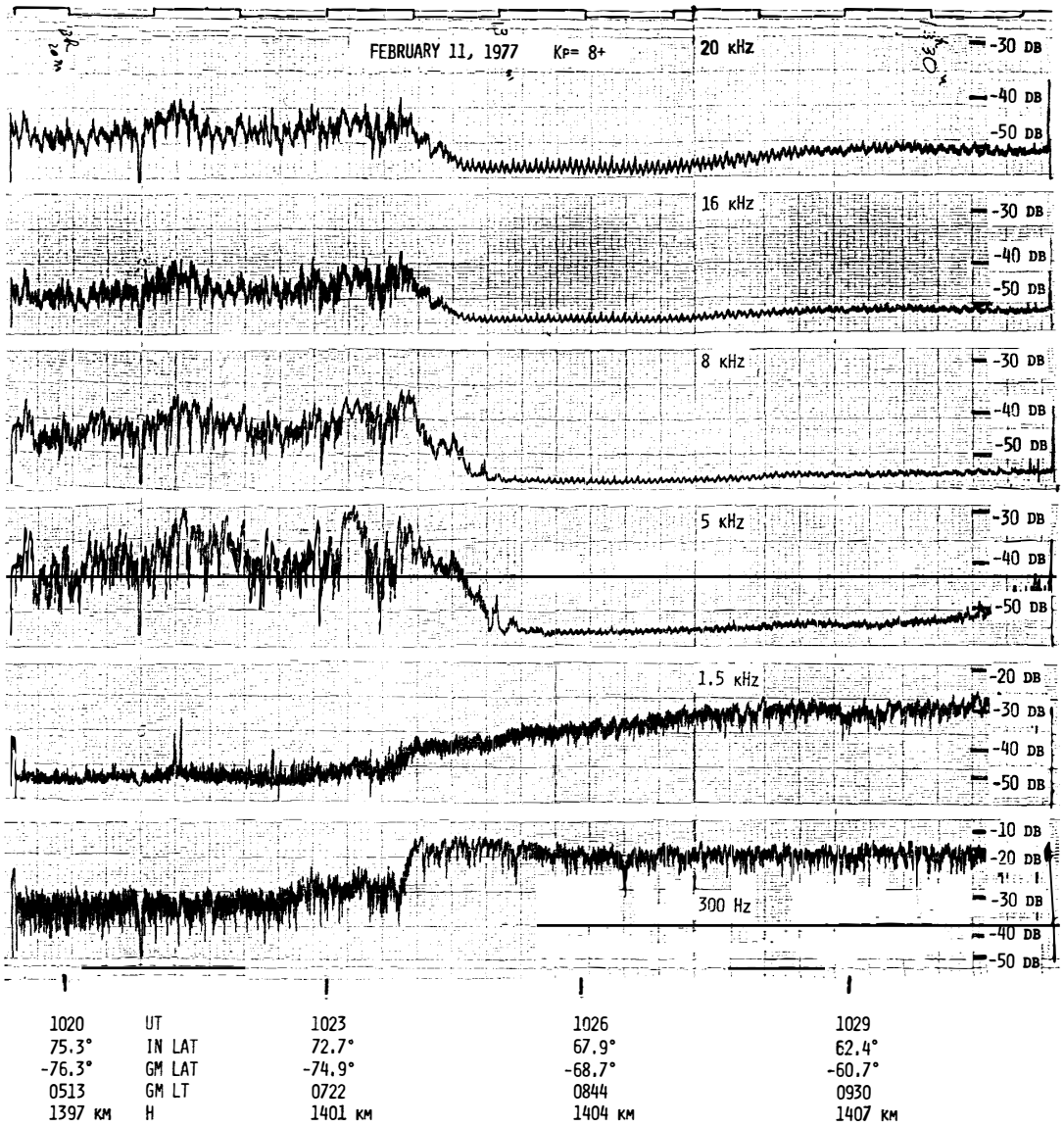
FEBRUARY 11, 1977 Kp= 8+
20 kHz
-30 DB
-40 DB
-50 DB
16 kHz
-30 DB
-40 DB
-50 DB
8 kHz
-30 DB
-40 DB
-50 DB
5 kHz
-30 DB
-40 DB
-50 DB
1.5 kHz
-20 DB
-30 DB
-40 DB
-50 DB
300 Hz
-10 DB
-20 DB
-30 DB
-40 DB
-50 DB
1020 UT 1023 1026 1029
75.3° IN LAT 72.7° 67.9° 62.4°
-76.3° GM LAT -74.9° -68.7° -60.7°
0513 GM LT 0722 0844 0930
1397 KM H 1401 KM 1404 KM 1407 KM

Fig. 1c.

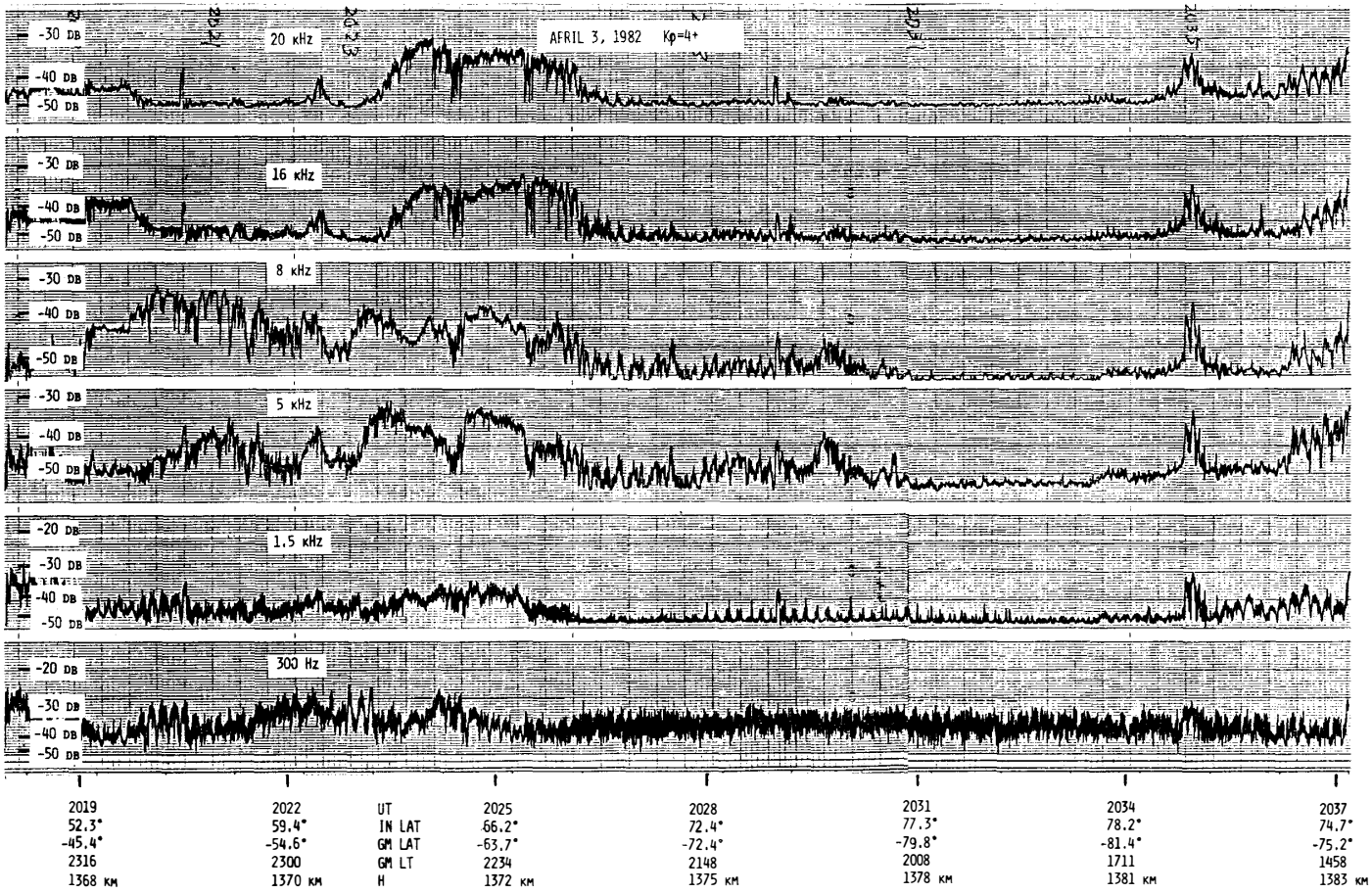

Fig. 2a.

Figs. 2a–2b. Examples of broad-band auroral hisses observed at high invariant latitudes above about 60° on ISIS passes of April 3, 1982, Kp=4+ (2a) and June 14, 1982, Kp=4 (2b).

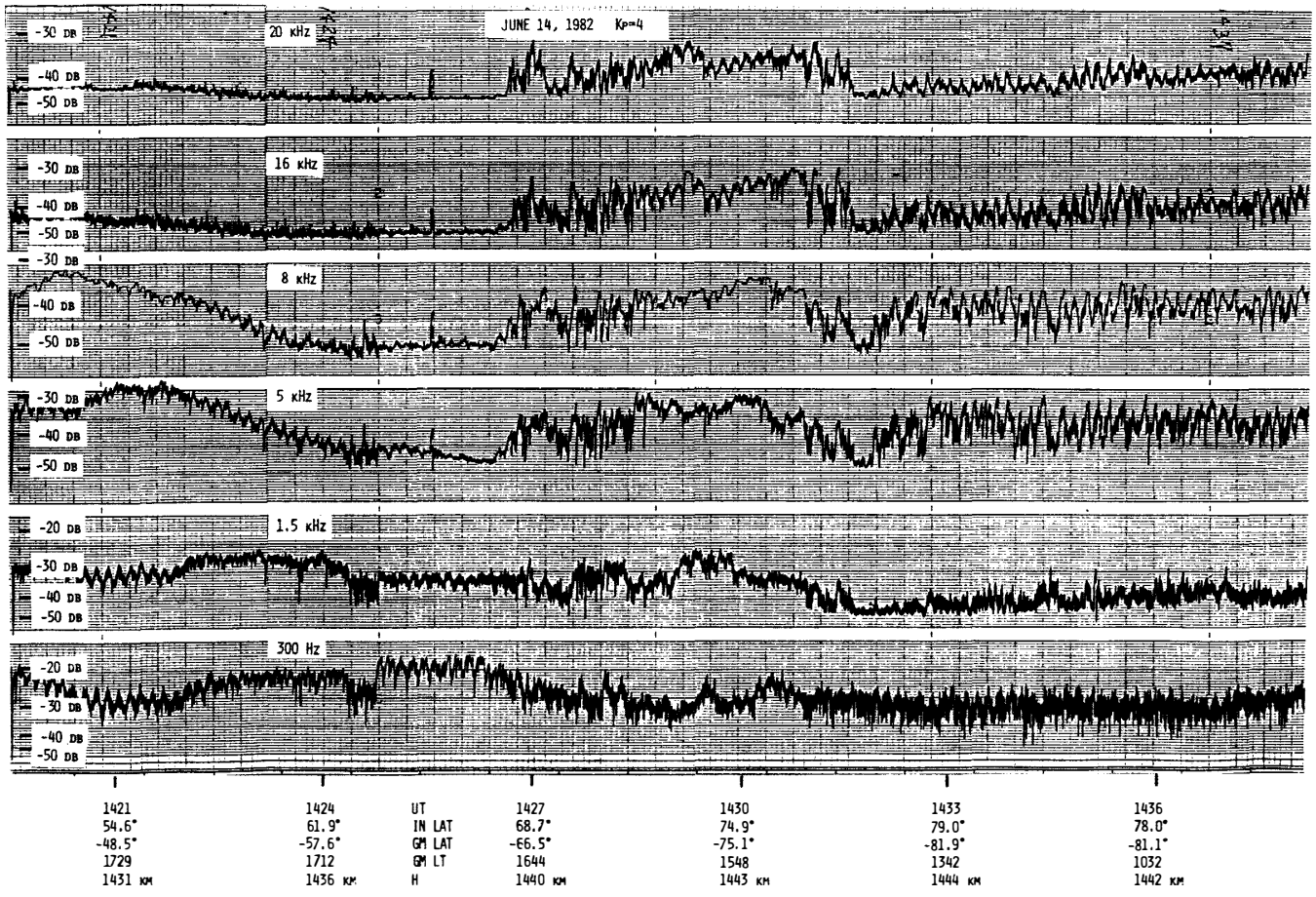
JUNE 14, 1982 Kp=4
20 kHz
16 kHz
8 kHz
5 kHz
1.5 kHz
300 Hz
-30 DB
-40 DB
-50 DB
-20 DB
1421 1424 1427 1430 1433 1436
UT
54.6° 61.9° IN LAT 68.7° 74.9° 79.0° 78.0°
-48.5° -57.6° GM LAT -66.5° -75.1° -81.9° -81.1°
1729 1712 GM LT 1644 1548 1342 1032
1431 KM 1436 KM H 1440 KM 1443 KM 1444 KM 1442 KM

Fig. 2b.

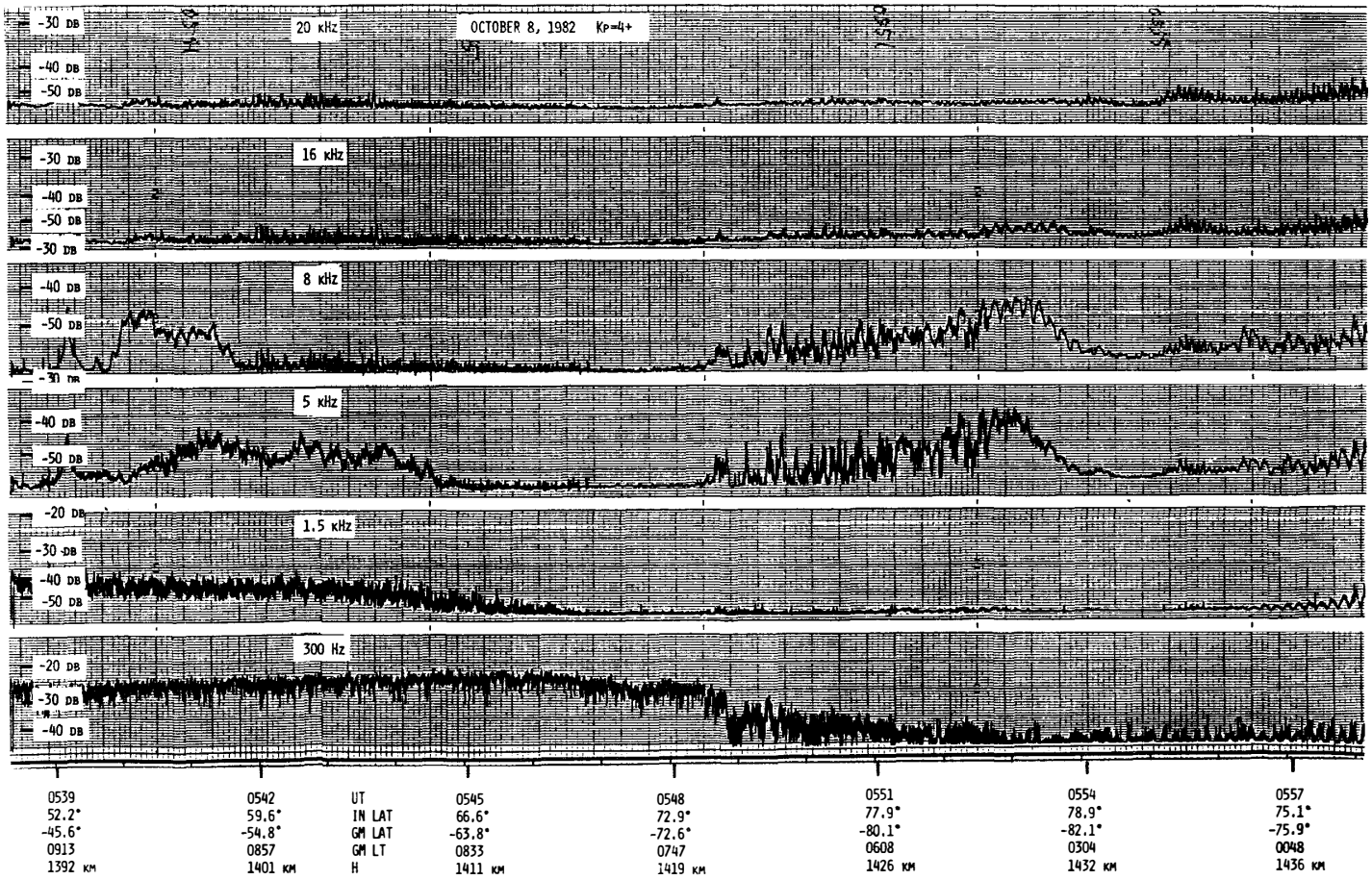

Fig. 3. An example of narrow-band auroral hiss in 5 and 8 kHz bands observed at invariant latitude between 73° and 79° in the local morning of October 8, 1982, Kp=4+ by ISIS-2.

than 25° in invariant latitude. We select ISIS-VLF passes with latitudinal extent more than 20° received at Syowa Station like Figs. 2a and 2b in order to have a uniform statistical-weight over all parts of the polar region in drawing an occurrence map of the broad-band auroral hiss. We define the broad-band auroral hiss with a criterion of simultaneous intensity increases above 5 dB as compared with the quiet-time level at 5, 8, 16 and 20 kHz bands in high invariant latitudes above 60° as shown by Figs. 2a and 2b. Figure 2b shows that broad-band auroral hisses occur at invariant latitudes higher than 67° and that, at invariant latitudes below 62°, mid-latitude VLF hiss appears at 5 and 8 kHz (ONDOH *et al.*, 1981). Also, in Fig. 2a, a broad-band auroral hiss occurs in 5, 8, 16 and 20 kHz bands at invariant latitudes between about 60° and 70°, and a mid-latitude VLF hiss occurs in 5 and 8 kHz bands at invariant latitudes below about 60°.

Figure 3 shows an occurrence of a narrow-band auroral hiss at 5 and 8 kHz bands at invariant latitudes between about 73° and 79°, but we exclude the narrow-band auroral hiss in drawing the occurrence map of the broad-band auroral hiss. We select 347 ISIS-VLF records like Figs. 2a and 2b received at Syowa Station from June 1976 to January 1983. Narrow-band VLF data as shown in Figs. 1–3 are taken from the Radio and Space Data Nos. 9, 13 and 15 (ONDOH *et al.*, 1981, 1983, 1984).

For a statistical analysis of occurrence frequency of broad-band auroral hiss, we define a unit area with invariant-latitude width of one degree and geomagnetic local time interval of one hour at high invariant latitudes above 60°. Then, the occurrence rate of broad-band auroral hiss in each area is defined by the ratio of ISIS pass number including broad-band auroral hiss to all ISIS pass number received over each area. The ISIS passes received over each area at invariant latitudes below 78° and at invariant latitudes between 78° and 80° amount to above 140 and from 80 to 100 respectively, but they are between 60 and 30 at invariant latitudes from 80° to 84°. So, the occurrence rates of broad-band auroral hiss at invariant latitudes between 80° and 84° are statistically less significant than those at latitudes below 80°.

Figures 4a and 4b show latitudinal variations of the occurrence rate of broad-band auroral hiss for local-time intervals of 3 h, from 6–9 to 15–18 h MT and from 18–21 to 3–6 h MLT respectively. In Fig. 4a, a peak occurrence rate appears at latitude 78°–80° for 6–9 h MLT, and at latitude 76°–78° from 9–12 to 15–18 h MLT. In Fig. 4b, a peak occurrence rate is seen at latitude 78°–80° for all local times from 18–06 h MLT. The high occurrence rate above 0.3 extends to lower latitudes below 70° in local times of 18–00 MLT, but it is confined within invariant latitudes between 74° and 82° in other local times.

Then, we plot the occurrence rates of broad-band auroral hiss on the polar geomagnetic coordinate viewed from above the north pole, though ISIS-VLF data used were observed over the Antarctica. Figure 5 shows the polar map of occurrence rate of broad-band auroral hiss as also estimated from Figs. 4a and 4b, where equicontours of occurrence rate of 0.3, 0.4 and 0.5 for the broad-band auroral hiss are illustrated in the polar coordinates of MLT *vs.* invariant latitude. The high-latitude contour of occurrence rate of 0.3 lies at invariant latitude of 82°–83° at all local times, while the low-latitude contour of 0.3 lies at invariant latitude of about 74° around 10 h MLT and it extends down to 67° around 22 h MLT. The low-latitude contour of

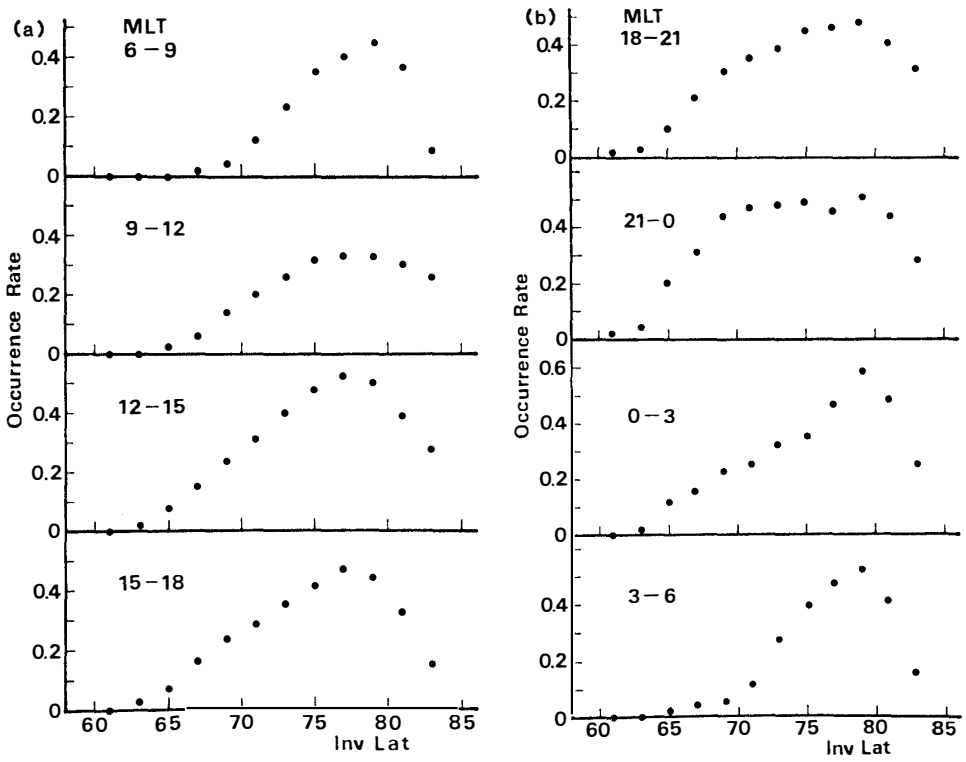

Figs. 4a–4b. Latitudinal dependence of occurrence rate of broad-band auroral hiss in each geomagnetic-local-time interval of 3 h, obtained from 347 ISIS-VLF passes received at Syowa Station, Antarctica from June 1976 to January 1983.

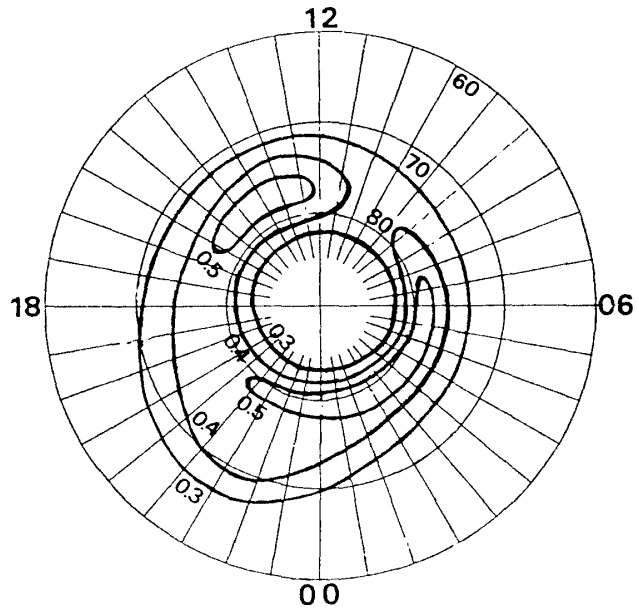

Fig. 5. Polar map of occurrence rate of broad-band auroral hiss obtained from Figs. 4a and 4b. The contours show occurrence rates of 0.3, 0.4 and 0.5 for broad-band auroral hiss.

occurrence rate of 0.3 is nearly symmetric with respect to the geomagnetic meridian of 10–22 h MLT. It is to be remarked here that the DP-2 current system showing the plasma convection pattern in the magnetospheric equatorial plane (NISHIDA, 1968)

has also the symmetric axis of 10–22 h MLT. However, regions of high occurrence rate above 0.5 are not always symmetric with respect to this meridian. They lie between 76° and 78° in the afternoon sector, and between 78° and 81° in the late night-morning sector.

4. Discussion on Polar Occurrence Map of Broad-band Auroral Hiss Observed by ISIS Satellites

The polar map of occurrence frequency of auroral hiss with magnetic field intensity above 10^{-12} gamma^2 Hz^{-1} at 9.6 kHz was shown by HUGHES *et al.* (1971) from VLF intensity data of Ariel-3. The Ariel VLF data used were observed in the maximum phase of sunspot cycle 20th. The inclination and orbital period of Ariel-3 are 80° and 96 min, respectively, with its altitude ranging from 500 to 600 km.

On the one hand, the polar map of occurrence rate of broad-band auroral hiss in Fig. 5 is derived from VLF electric field data (50 Hz–30 kHz) of ISIS-1 and ISIS-2 received at Syowa Station, Antarctica. The ISIS VLF data used were observed from the minimum to declining phase of sunspot cycle 21st. The inclination, period, perigee altitude and apogee altitude of ISIS-1 orbit are 88.4°, 128 min, 550 km and 3500 km respectively. Also these parameters of ISIS-2 orbit are 88.2°, 113.5 min, 1350 km and 1450 km respectively.

Figure 5 is considerably different from the occurrence map of 9.6 kHz auroral hiss which shows a pronounced dawn-dusk asymmetry with a distinct minimum in the auroral hiss occurrence in the local morning from about 2 to 8 h MLT (Fig. 6).

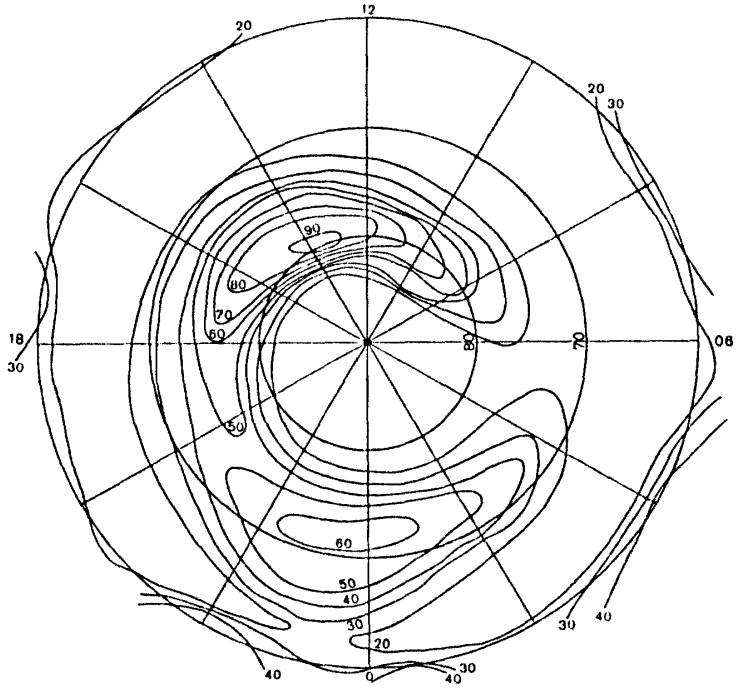

Fig. 6. Polar map of occurrence frequency of auroral hiss at 9.6 kHz as a function of invariant latitude and magnetic local time. Only events with magnetic field intensities above 10^{-12} gamma^2 Hz^{-1} are counted (after HUGHES et al., 1971).

The satellite altitude does not seem to affect the occurrence map of auroral hiss, since the both polar maps of auroral hiss occurrence are drawn on the polar coordinate of invariant latitude *vs.* geomagnetic local time, and since the auroral hiss propagates approximately along geomagnetic field lines on the whistler mode from altitudes above 4000 km. The auroral hiss observed in the topside ionosphere shows an electrostatic nature, such as the LHR frequency, especially at very low frequencies below a few kHz. Hence, any difference between wave magnetic field of Ariel data and wave electric field of ISIS data cannot be found on the both polar maps since the both maps of auroral hiss occurrence are obtained from VLF data at frequencies above 9 kHz. The polar occurrence map of broad-band auroral hiss (Fig. 5) has no dawn-dusk asymmetry in the auroral hiss occurrence as discussed above.

Next, we examine effects of auroral particle precipitation upon the occurrence maps of the auroral hiss as the Ariel result is derived from VLF data observed in the maximum phase of solar activity and the ISIS result is obtained from VLF data observed in the minimum to declining phase of solar activity.

In high-latitude magnetosphere, precipitating electrons are free energy sources for certain plasma instabilities. High-latitude particle precipitation is traditionally broken into three regions of the auroral oval, dayside cusp and polar cap.

Correlative studies have clearly indicated that strong auroral VLF hiss and auroral kilometric radiation occur simultaneously with inverted-V events in the auroral oval and on the low-latitude side of the polar cap (HOFFMAN and LAASPERE, 1972; GURNETT and FRANK, 1972; GREEN *et al.*, 1979). If one maps the region of inverted-V events along geomagnetic field lines, the occurrence region would correspond to the plasma sheet and magnetotail. Inverted-V events in the auroral oval are usually much more energetic than those in the polar cap. Many inverted-V events in the dusk-to-midnight hemisphere have been found to have a maximum peak energy greater than 10 keV. In the polar cap, the inverted-V's usually had much smaller peak energies from several hundred eV to about 1 keV (LIN and HOFFMAN, 1982).

Electrons of a few keV from the central plasma sheet precipitate into the region of diffuse aurora and their precipitations usually show a smooth dependence on locality and they produce diffuse auroral patterns. The diffuse auroral region lies approximately in the equatorial-side half of the auroral oval (AKASOFU, 1981). Particle precipitation near the high latitude boundary of the auroral oval, referred to as boundary plasma sheet precipitation, is characterized by discrete structures. The average energy of boundary plasma sheet electrons is typically a few hundred eV in quiet times and it increases dramatically during substorm periods (OSSAKOW *et al.*, 1984).

Inverted-V events occur essentially all the time, independent of geomagnetic activity (HOFFMAN and LIN, 1981), and the occurrence of the inverted-V events was independent of the altitude between 200 and 800 km (LIN and HOFFMAN, 1982). However, the low latitude boundary of occurrence depends strongly on local time, giving the impression of following the auroral oval. The mean latitudinal width of inverted-V events is about 0.5° invariant latitude and the average longitudinal extension appears to be much greater than the typical width, 0.1° of auroral arcs.

The energy spectra of inverted-V precipitating electrons consist of two components: monoenergetic electron beams and backscattered secondary electrons which

are produced by collisions of monoenergetic electrons with the atmosphere below 200 km. Statistically the maximum peak energy of an inverted-V event is much higher from 19 to 01 h MLT (above 5 keV), whereas the maximum peak energy for the other local times is about 1 keV. The average of the maximum peak energy of inverted-V events is 2 keV for geomagnetic local time of 3–7 h and 3.5 keV for 16–20 h (LIN and HOFFMAN, 1982). This is the only one dawn-dusk asymmetry of the inverted-V event. But this asymmetry cannot cause the pronounced dawn-dusk asymmetry in the occurrence map of 9.6 kHz auroral hiss.

HUGHES *et al.* (1971) used a criterion of the auroral hiss with magnetic field above 10^{-12} gamma^2 Hz^{-1} at 9.6 kHz to derive the occurrence map of 9.6 kHz auroral hiss, but this criterion seems to take up relatively strong auroral hisses, since the quiet-time intensity of auroral hiss observed by Ariel satellites is of the order of 10^{-15} gamma^2 Hz^{-1}. So, it seems plausible that HUGHES *et al.* (1971) showed the occurrence map of relatively strong auroral hiss by using the fixed frequency (9.6 kHz) VLF data, while the occurrence map of broad-band auroral hiss is obtained from the multi-frequency ISIS data of average auroral VLF hiss.

In summary, the auroral VLF hiss seems to be generated by structured electron precipitation, such as inverted-V electrons, from the boundary plasma sheet. The occurrence of inverted-V events has no pronounced dawn-dusk asymmetry and also has no dependence on the geomagnetic *Kp* index and the data acquisition altitude. Thus, properties of the inverted-V event related to the auroral VLF hiss suggest that the solar activity or geomagnetic activity and data acquisition altitude do not give a significant effect on the occurrence map of auroral VLF hiss, although auroral particle precipitations depend generally on the solar activity cycle and also the geomagnetic activity.

The discrepancy between the Ariel and ISIS results seems to be due to a difference in the VLF magnetic field data of fixed frequency and VLF electric field data of multi-frequencies as discussed in reference to Figs. 1–3, because a detection probability of

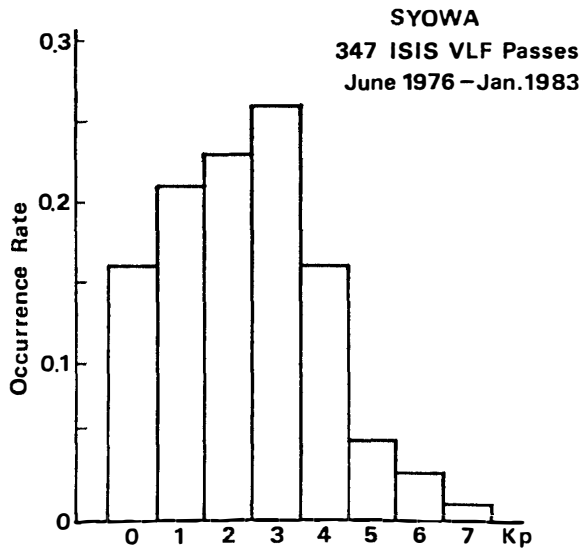

Fig. 7. Kp-dependence of occurrence rate of 347 ISIS passes received at Syowa Station, Antarctica from June 1976 to January 1983.

auroral hiss by ISIS multi-frequency data is much higher than that by Ariel fixed-frequency data.

Figure 7 shows *Kp* dependence of the occurrence rate of 347 ISIS-VLF passes used for deriving Figs. 4–5. Geomagnetic activities for most ISIS-VLF passes used are below $Kp=4$, so that Fig. 5 seems to represent the average condition of auroral hiss occurrence.

5. Conclusion

Narrow-band VLF intensity data at six frequencies are processed from magnetic tapes of ISIS-VLF electric field (50 Hz–30 kHz) data received at Syowa Station, Antarctica. We define a broad-band auroral hiss with a criterion of simultaneous intensity increases above 5 dB as compared with the quiet-time level at 5, 8, 16 and 20 kHz bands of the narrow-band ISIS-VLF data observed at invariant latitudes above 60°. Broad-band auroral hisses were detected clearly between 04 and 09 h MLT at invariant latitudes from 72° to 75° for various geomagnetic activities in contrast with the distinct morning minimum of auroral hiss occurrence at 9.6 kHz obtained by HUGHES *et al.* (1971). Also the occurrence rate of broad-band auroral hiss in each area with latitudinal width of one degree and local time interval of one hour is defined by the ratio of the number of ISIS passes including the broad-band auroral hiss to the total number of ISIS passes over each area. A polar map of occurrence rate of broad-band auroral hiss is obtained by plotting occurrence rates of broad-band auroral hiss on the polar coordinate of invariant latitude *vs.* geomagnetic local time viewed from above the north pole, using narrow-band VLF intensity data of 347 ISIS-VLF passes received at Syowa Station from June 1976 to January 1983. The high-latitude contour of occurrence rate of 0.3 lies approximately along the latitudinal circle of 82°. The region of occurrence rate of 0.3 extends down to 67° around 22 h MLT and to 74° around 10 h MLT, and it is symmetric with respect to the 10–22 h MLT meridian, but the regions of high occurrence rate above 0.5 are not at all symmetric with respect to that meridian. They are located between 76° and 78° in the afternoon sector and between 78° and 81° in the late night–morning sector. The occurrence map of broad-band auroral hiss does not show any dawn-dusk asymmetry as shown in the occurrence map of 9.6 kHz auroral hiss. The discrepancy between the occurrence maps of auroral VLF hiss obtained from the Ariel VLF magnetic field and the ISIS-VLF electric field data is discussed in terms of auroral particle precipitation, VLF data used, data analysis method and telemetry coverage of receiving stations.

The following two reasons are suggested as causes of the discrepancy: The Ariel result is obtained from the fixed frequency VLF intensity data, while the multi-frequency VLF intensity data are used in the ISIS result, and the Ariel result takes up relatively strong auroral hisses as compared with the ISIS result.

References

AKASOFU, S.-I. (1981): Auroral arcs and auroral potential structure. Physics of Auroral Arc Formation, ed. by S.-I. AKASOFU and J. R. KAN. Washington, D. C., Am. Geophys. Union, 1–14

(Geophys. Monogr., 25).

DUNCAN, R. A. and ELLIS, G. R. (1959): Simultaneous occurrence of sub-visual auroræ and radio noise bursts on 4.6 kc./s. Nature, **183**, 1618–1619.

ELLIS, G. R. (1957): Low-frequency radio emission from aurorae. J. Atmos. Terr. Phys., **10**, 302–306.

GREEN, J. L., GURNETT, D. A. and HOFFMAN, R. A. (1979): A correlation between auroral kilometric radiation and inverted V electron precipitation. J. Geophys. Res., **84**, 5216–5222.

GURNETT, D. A. (1966): A satellite study of VLF hiss. J. Geophys. Res., **71**, 5599–5615.

GURNETT, D. A. and FRANK, L. A. (1972): VLF hiss and related plasma observations in the polar magnetosphere. J. Geophys. Res., **77**, 172–190.

HARANG, L. and LARSEN, R. (1965): Radio wave emissions in the v.l.f.-band observed near the auroral zone—I; Occurrence of emissions during disturbances. J. Atmos. Terr. Phys., **27**, 481–497.

HELLIWELL, R. A. (1965): Whistlers and Related Ionospheric Phenomena, Stanford, Stanford University Press, 349 p.

HOFFMAN, R. A. and LAASPERE, T. (1972): Comparison of very-low-frequency auroral hiss with precipitating low-energy electrons by the use of simultaneous data from two Ogo 4 experiments. J. Geophys. Res., **77**, 640–650.

HOFFMAN, R. A. and LIN, C. S. (1981): Study of inverted-V auroral precipitation events. Physics of Auroral Arc Formation, ed. by S.-I. AKASOFU and J. R. KAN. Washington D. C., Am. Geophys. Union, 80–90 (Geophys. Monogr., 25).

HUGHES, A. R. W., KAISER, T. R. and BULLOUGH, K. (1971): The frequency of occurrence of VLF radio emissions at high latitudes. Space Research XI, ed. by K. Ya. KONDRATYEV *et al.* Berlin, Akademie, 1323–1330.

JØRGENSEN, T. S. and UNGSTRUP, E. (1962): Direct observation of correlation between auroræ and hiss in Greenland. Nature, **194**, 462–463.

LIN, C. S. and HOFFMAN, R. A. (1982): Observations of inverted-V electron precipitation. Space Sci. Rev., **33**, 415–457.

MARTIN, L. H., HELLIWELL, R. A. and MARKS, K. R. (1960): Association between auroræ and very low-frequency hiss observed at Byrd Station, Antarctica. Nature, **187**, 751–753.

MOROZUMI, H. M. (1963): Semi-diurnal auroral peak and VLF emissions observed at the south pole. Trans. Am. Geophys. Union, **44**, 798–806.

NISHIDA, A. (1968): Geomagnetic $D_p 2$ fluctuations and associated magnetospheric phenomena. J. Geophys. Res., **73**, 1795–1803.

ONDOH, T. (1963): The ionospheric absorption of the VLF emissions at the auroral zone. J. Geomagn. Geoelectr., **15**, 90–108.

ONDOH, T., NAKAMURA, Y., WATANABE, S. and MURAKAMI, T. (1981): Narrow-band 5 kHz hiss observed in the vicinity of the plasmapause. Planet. Space Sci., **29**, 65–72.

ONDOH, T., NAKAMURA, Y., WATANABE, S. and MURAKAMI, T. (1981; 1983; 1984): ISIS VLF data received at Syowa Station, Antarctica. Radio and Space Data, **9**, 244 p.; **13**, 245 p.; **15**, 117 p.

OSSAKOW, S., BURKE, W., CARLSON, H. G., GARY, P. HEELIS, R., KESKINEN, M., MAYNARD, N., MENG, C., SZUSZCZEWICZ, E. and VICKREY, J. (1984): High latitude ionospheric structure. Solar Terrestrial Physics: Present and Future, ed. by D. M. BUTLER and K. PAPADOPOULOS. Washington, D. C., NASA, 12.1–12.39 (NASA Ref. Publ., **1120**).

(Received May 7, 1987; Revised manuscript received September 24, 1987)